Applied Catalysis B: Environmental 98 (2010) 161–170

Contents lists available at ScienceDirect

Applied Catalysis B: Environmental

journal homepage: www.elsevier.com/locate/apcatb

Preferential oxidation of CO catalyzed by supported polymer-protected palladium-based nanoparticles

Izaskun Miguel-García, Ángel Berenguer-Murcia *, Diego Cazorla-Amorós

Departamento de Química Inorgánica, Universidad de Alicante, Ap. 99, E-03080 Alicante, Spain

ARTICLE INFO

Article history:
Received 20 February 2010
Received in revised form 19 May 2010
Accepted 24 May 2010
Available online 31 May 2010

Keywords:
Preferential oxidation of CO (PrOx)
Noble metal nanoparticles
Alumina
Hydrogen purification

ABSTRACT

Palladium nanoparticles protected by polyvinylpyrrolidone (PVP) have been synthesized by the reduction-by-solvent method and deposited on alumina by impregnation. The prepared catalysts have been tested in the preferential oxidation of carbon monoxide (PrOx) in H_2-rich gaseous streams and the results have been compared with catalysts prepared by conventional impregnation. Pd-nanoparticles protected by PVP have good activity and outstanding selectivity towards CO oxidation (above 50% in some cases). On the contrary, the impregnated catalyst has very low selectivity (about 10%). The influence of crucial parameters such as the capping agent-to-metal ratio or the synthesis temperature of the nanoparticles on the catalytic performance of the prepared materials has been analyzed. Our results show that within the 2.5–3.5 nm region, particle size of supported nanoparticles does not seem to exert a significant influence on the studied reaction. However, the amount of capping agent seems to be crucial to prepare efficient, stable catalysts. The samples prepared show 100% CO removal at 180 °C when tested in the presence of CO_2 and water vapour.

1. Introduction.

The synthesis and utilization of nanomaterials in applications such as catalysis, sensor development, energy storage, and biomedical applications requires knowledge of a variety of properties, the most important of which are size and structure. Within this field, nanoparticles have shown great potential in a wide range of reactions such as selective oxidations using noble metal nanoparticles in liquid phase [1,2] and selective hydrogenations using mono [3] and multimetallic [4,5] nanoparticles. During the past two decades, significant efforts have been dedicated to the preparation of both metallic and metal oxide nanoparticles [6–8], resulting in substantial progress in tuning their size and shape [9]. These two parameters are well-known to have a strong influence on their subsequent catalytic properties. In particular, the surface capping agent may have a strong effect on catalytic activity and selectivity, as some studies have already indicated for some noble metal nanoparticles [10,11].

Immobilization of catalytic species on a selected support is of great interest in modern chemical industry. In heterogeneous catalysis, one of the key aspects lies in the preparation of the catalyst itself. The size and composition of the catalytically active particles are difficult to control despite the number of existing and reported procedures which could be labelled as "classical" [12]. In this sense, nanoparticle synthesis might result in a promising alternative to traditional methods, since it allows a very precise control of both the particle size [13] and final composition [4] of the resulting materials.

In the current economic scenario, hydrogen is unfolding into a key energy vector for the development of clean, efficient fuels [14]. Nowadays, hydrocarbon reforming is the most widely used industrial process to produce hydrogen [15]. In this respect, mobile devices may carry a reformer on board to generate the fuel *in situ*. Nevertheless, it must be noted that some compounds such as carbon monoxide and sulfur are present in the effluent coming from the reformer. Such gases may poison the Pt catalyst present in the anode of the fuel cell. Thus, concentrations lower than 10 ppm and 10 ppb respectively are needed to avoid poisoning [16]. Water-gas shift (WGS) has been successfully applied to the removal of sulfur, but concentrations of carbon monoxide between 1000 and 10,000 ppm are still present in the gaseous stream [14].

Oxidation to the corresponding dioxide clearly stands as an option for the removal of carbon monoxide. In the case of mobile devices, the gases emerge from the WGS reactor at a temperature around 200 °C. Thus, the ideal catalyst should be one that, operating at temperatures close to 200 °C, remains stable for long periods of time while showing good reusability. Many reports have described the oxidation of CO over Au catalysts supported on different metal oxides [17–19]. However, these catalysts are only active at low tem-

* Corresponding author. Tel.: +34 965 909350; fax: +34 965 903454.
E-mail address: a.berenguer@ua.es (Á. Berenguer-Murcia).

0926-3373/$ – see front matter © 2010 Elsevier B.V. All rights reserved.
doi:10.1016/j.apcatb.2010.05.025

perature (200 K), and strongly deactivate at higher temperatures [20,21].

On the other hand, the oxidation of carbon monoxide has been extended to other metals such as silver, chromium, copper, palladium, rhodium or platinum (see, for example, Refs. [22–26]) following various preparation protocols. More recent studies have analyzed the potential of using protected metallic nanoparticles in the oxidation of CO [10,27], although there is still a lot of ground to explore in this field.

Thus, the aim of this work is to prepare polymer-protected palladium nanoparticles with different particle sizes by modifying synthetic parameters such as polymer load or reaction temperature and deposit them by the impregnation method. The prepared catalysts will be tested in the PrOx reaction in a H_2-rich feed and the results will be compared with those of catalysts prepared by a conventional impregnation method. We will analyze the evolution of the catalytic activity over a range of temperatures, and the data will be critically compared and put into perspective with the results by other research groups.

2. Experimental

2.1. Synthesis of nanoparticles

Pure palladium nanoparticles were synthesized following the reduction-by-solvent method [4,28], adapting a previously published procedure [29–31].

The nanoparticles precursor salt was $Pd(ac)_2$ (98%, Sigma–Aldrich), and polyvinylpirrolidone was used as the capping agent (PVP, 40 K, Sigma–Aldrich). The reaction was carried out in an inert atmosphere using a Schlenk system, according to the following procedure.

Solution 1: 1.114 g (10 mmol) of protective polymer were weighted and transferred to a three-necked round bottom flask containing 120 mL of ethylene glycol. The solution was stirred vigorously at 80 °C for 2 h, using a magnetic stirrer and an oil bath.

Solution 2: 0.2245 g (1 mmol) of the palladium precursor were weighted and added to 50 mL of dioxane. The solution, light orange in colour, was stirred for two hours at room temperature using a magnetic stirrer.

Solution 1 was cooled to 0 °C, and 3 mL of 1 M sodium hydroxide solution were added under stirring. Solution 2 was then poured on solution 1 under vigorous stirring, and the resulting mixture was heated at 100 °C for 2 h. After a few minutes, the colour of the solution changed from light orange to dark brown, indicating the formation of metallic zerovalent nanoparticles [4].

As we have previously reported [29], the resulting colloidal suspension is stable against sintering, and the nanoparticles can be stored at ambient conditions without formation of aggregates.

Under the conditions stated here, different synthesis temperatures, amounts of precursors and solvents have been employed in order to synthesize nanoparticles with different sizes.

2.2. Purification of the nanoparticles

In order to prepare the catalysts, the palladium nanoparticles were purified (i.e. removed from the excess capping agent, high-boiling point solvent, and salts used in the synthesis) and redispersed in methanol.

For the purification, an aliquot (50 mL) of the as-synthesized colloid was poured into a 1 L glass bottle, and a large excess of acetone (~600 mL) was added. The solution was vigorously shaken and left to settle until flocculation of the particles occurred. The supernatant was then discarded, and the aggregated nanoparticles were redispersed in the adequate amount of methanol, thus obtaining a suspension of perfectly known concentration.

2.3. Preparation of the catalysts

The catalysts used in this work were prepared by the impregnation method, as reported previously by our group [30,31]. In a typical synthesis, 1 g of the support (γ-Al_2O_3, pellets, Sigma–Aldrich, 99%) was ground to a fine powder in an agate mortar and mixed with the appropriate amount of the purified colloid suspension to yield a 1% wt. of metallic loading. The solution was vigorously stirred for two days in order to ensure similar load and dispersion in the different catalysts, and transferred to an oven, where it was left at 60 °C in order to evaporate the methanol. The catalyst was then washed several times with a cold mixture of H_2O/EtOH (50:50, v/v), and left to dry overnight at 60 °C. The prepared catalysts were ground and stored under ambient conditions.

In order to critically compare the catalytic results of our nanoparticle-based catalysts, a standard catalyst was also prepared by the "classical" impregnation method [24,32–34].

For its preparation, the appropriate amount of $Pd(ac)_2$ (21.1 mg, 0.094 mmol) was dissolved in the minimum amount of dioxane (3.5 mL) and stirred for 12 h. The solution was then mixed with the support (1 g Al_2O_3), and the resulting suspension was stirred for 8 h. The mixture was dried at 60 °C overnight. The sample was calcined at 500 °C for 4 h (heating rate 5 °C/min). The heat-treated catalyst was stored under ambient conditions.

All catalysts were submitted to a reductive treatment prior to testing their catalytic activity in order to ensure complete reduction of the metal in the catalyst. Thus, each sample was reduced at 200 °C for 2 h (heating rate 5 °C/min) in 10% H_2 in He (100 mL/min), as indicated by TPR experiments carried out in our laboratories. This pre-treatment does not affect the capping agent significantly, as the polymer decomposition starts above 400 °C [35]. The nanoparticle catalysts were also submitted to this pre-treatment in order to critically compare the catalytic results.

2.4. Characterization of the catalysts

TEM images of the catalysts were recorded in an electron microscope JEOL (JEM-2010) equipped with an EDS analyzer (OXFORD, model INCA Energy TEM 100) operating at 200 kV with a space resolution of 0.24 nm. For the analysis, a small amount of the catalyst was suspended in a few drops of ethanol, and sonicated for a few minutes. A drop of this suspension was then deposited onto a 300 mesh Lacey copper grid and left to dry at room temperature.

The diameter of the nanoparticles (d) was estimated directly from the micrographs, by counting a minimum of 100 particles. The average value of the palladium particle diameters was calculated by the following equation, where n_i is the number of particles of diameter d_i [29].

$$d \approx \frac{\sum n_i d_i}{\sum n_i}$$

The dispersion of metal over the catalyst (D) was estimated according to the following equation, assuming spherical shape for the particles [36].

$$D \approx \frac{0.9}{d\,(\mathrm{nm})}$$

The metal loading of the catalysts was analyzed before and after the reaction cycles by inductively coupled plasma-optical emission spectroscopy (ICP-OES), in a PerkinElmer Optima 4300 system. The extraction of the metal was made by an oxidative treatment of the samples with aqua regia, followed by filtration of the remain-

Table 1
Synthesis conditions of the different palladium colloids presented in this study.

Sample	T. synthesis (°C)	PVP/Pd ratio (mol/mol)	*d* TEM (nm)
Pd-1	0	10	2.5 ± 0.5
Pd-2	50	10	2.4 ± 0.5
Pd-3	100	10	2.2 ± 0.4
Pd-4	150	10	2.4 ± 0.5
Pd-5	100	0.1	[a]
Pd-6	100	1	3.6 ± 0.8
Pd-7	100	50	2.4 ± 0.7
Pd-8[b]	100	10	2.5 ± 0.5
Pd-9[c]	100	10	4.3 ± 0.7

[a] This sample showed heavy cluster formation, which prevented reliable particle size determination.
[b] Solvent amount was reduced by a factor of two in the synthesis, so that Pd concentration was two times higher than the method described in Section 2.
[c] Solvent amount was reduced by a factor of five in the synthesis, so that Pd concentration was five times higher than the method described in Section 2.

ing solid using a nylon membrane filter (average pore diameter 400 nm) and dilution of the resulting metal solution using a volumetric flask.

X-ray photoelectron spectroscopy (XPS) data were recorded using a VG-Microtech Multilab 3000 spectrometer. Thermogravimetric analyses of the samples were performed in a SDT 2960 Simultaneous DSC–TGA system, by TA Instruments, with a heating rate of 20 °C/min, under 100 ml/min of He flow.

2.5. Catalytic tests

The prepared catalysts were tested in the preferential oxidation of CO. Prior to reaction, the samples were reduced as previously described. The reactor was a U-shaped quartz reactor (16 mm inner diameter), where the catalytic activity of 150 mg of sample was tested under flow conditions. The reactant gas composition (2% CO, 2% O_2, 30% H_2, balance He) is a hydrogen-rich feed similar to that exiting the water-gas shift reactor in the H_2 purification process for fuel cell applications, as other authors have indicated [34,37,38]. The most promising catalyst was tested under more realistic conditions, where water vapour and carbon dioxide were also fed to the reactor inlet feed to obtain the following composition: 2% CO, 2% O_2, 30% H_2, 5% H_2O, 20% CO_2, balance He. Non-isothermal experiments were done using a heating rate of 2 °C/min and a total gas flow rate of 100 mL/min that was set by means of Mass Flow Controllers (MFCs, Bronkhorst). The resulting space velocity was 30,000 h^{-1}, although different space velocities were used in some specific cases in order to optimize CO conversion and reach 100% CO conversion, thus proving the validity of these catalysts to remove CO. Isothermal experiments were also performed to determine the reaction rates and activation energies. Reaction rates are expressed as moles of CO consumed per gram of Pd metal per second, and as TOF (in s^{-1}), defined as moles of CO consumed per mole of surface metal per second. Activation energies were calculated from isothermal experiments at conversions lower than 20%. The exhaust gases were analyzed by gas chromatography (Agilent Technologies 6890N equipped with a carbon-PLOT column operating at 30 °C and a TCD detector).

Conversion and selectivity in the reactions were calculated as follows:

$$\text{Conv. CO}\,(\%) = \frac{[\text{CO}]_0 - [\text{CO}]}{[\text{CO}]_0} \times 100$$

$$\text{Conv. O}_2\,(\%) = \frac{[\text{O}_2]_0 - [\text{O}_2]}{[\text{O}_2]_0} \times 100$$

$$\text{Selectivity}\,(\%) = \frac{[\text{CO}]_0 - [\text{CO}]}{[\text{O}_2]_0 - [\text{O}_2]} \times 50$$

Table 2
TEM results and metal loading of the different catalysts.

Sample	*d* TEM (nm)	*D* TEM (%)	Metal loading ICP (%)
Pd/A-1	4.2 ± 1.1	21	0.53
Pd/A-2	3.0 ± 0.5	29	0.69
Pd/A-3	2.8 ± 0.6	32	0.40
Pd/A-4	3.4 ± 1.1	26	0.71
Pd/A-5	[a]	–	0.85
Pd/A-6	3.6 ± 0.8	25	0.39
Pd/A-7	3.0 ± 0.7	29	0.44
Pd/A-8	3.2 ± 0.7	28	0.54
Pd/A-9	4.6 ± 0.7	20	0.43
Pd/A-Impregnation	3.9 ± 1.5	23	0.52

[a] This sample showed heavy aggregation which prevented reliable particle size determination.

Selectivity was calculated from the non-isothermal experiments. In this respect, catalytic experiments carried out in absence of CO revealed that these systems are highly active for H_2 oxidation (100% oxygen consumption occurred at room temperature), as expected. T_{50}, defined as the temperature at which CO conversion reached 50% for each sample, was also used as a parameter to assess the performance of the catalysts.

3. Results and discussion

3.1. Catalysts characterization

Several colloids were synthesized at different reduction temperatures, and with different capping agent/metal ratios. The effect of the concentration of metal species was also considered.

Table 1 shows a brief summary of the preparation protocol for each colloid, which were used (upon purification) to prepare the catalysts. These are named after the colloids, taking into account the support used in this case. Thus, catalyst Pd/A-1 corresponds to colloid Pd-1 supported on Al_2O_3.

Fig. 1 shows the TEM images of different colloids prepared for this work. As it can be extracted from the TEM micrographs, the synthesis temperature does not seem to exert a significant influence on the observed size of the palladium particles (colloids Pd-1 to Pd-4). The synthesized colloids show very low polydispersity in the size of the particles, which might be partially attributed to the high amount of capping agent present in the reaction medium. Too high reduction temperatures may involve very fast nanoparticle nucleation and growth kinetics, which would be undesirable since the nanoparticle synthesis conditions would be less controlled. This ultimately results in the particle size reaching values close to 10 nm when the reduction is carried out in ethylene glycol at 180 °C.

The role of the amount of protecting agent present in the reaction medium is also important when reduction of the metal cations takes place [13,39,40]. Proceeding from a low (0.1) PVP/Pd ratio (sample Pd-5), the nanoparticles evolve from large nanoparticulate aggregates with sizes of several tens of nanometers to small aggregates formed by 3–4 nanoparticles of approximately 5 nm in size (PVP/Pd = 1, sample Pd-6) to individual, isolated nanoparticles (PVP/Pd = 10–50, samples Pd-3 and Pd-7). There is an upper threshold for the PVP concentration over which no decrease in the average particle size is observed for polyol-reduced Pd nanoparticles. This is confirmed by the similarity in size of the particles observed in samples Pd-3 and Pd-7, prepared with PVP/Pd ratios of 10 and 50, respectively.

As we have observed in previous works [30,31], deposition of the polymer-protected nanoparticles may bring forth a noticeable change in the particle size. Fig. 2 shows the TEM images of the different catalysts prepared for this work.

Table 2 shows the diameter of the particles (*d*) after deposition on the supports and the dispersion (*D*) calculated from the TEM

analysis of the different catalysts prepared. According to our previous study, TEM may be considered a reliable tool to estimate the average size of colloidal nanoparticles (and hence their dispersion) [29,30].

TEM micrographs show an effect on the size of the particles during catalyst preparation, as the mean particle size slightly increases from the starting colloid to the final catalyst. Although aggregates of particles are not apparent during TEM analysis, some agglomeration during catalyst preparation cannot be ruled out. The case of Pd/A-1 presents the highest relative increase in nanoparticle size when the colloid is deposited on the alumina support. Considering that the synthesis temperature of the colloid was 0 °C, the PVP chains might be too stiff to efficiently surround the growing nanoparticles, rendering them more susceptible to agglomeration during deposition. This increase in size could also be related to the change of shape of the particles. This change, from spherical in the colloid, to ellipsoidal in the catalysts due to deposition, may be the cause of the apparent change of size, and is clearly visible in the inset of Fig. 2B.

TEM analyses were performed on several samples after reaction (results not shown) in order to assess any possible deactivating effects on the catalysts over time under reaction conditions, with no significant change either in the size or the shape of the nanoparticles compared to the fresh samples. Plasma analyses performed on the catalysts after reaction in order to determine any possible loss of Pd in the catalysts revealed no leaching due to reaction conditions. TG analyses performed on several fresh samples showed that no significant degradation of the polymer occurs in the samples in the temperature interval analyzed in the catalytic tests. Fig. 3 shows the thermal decomposition process for pure PVP and samples Pd/A-3 and Pd/A-4. All the other Pd colloidal catalysts have similar decomposition profiles (results not shown). It can be observed that minor degradation of the polymer occurs at 200 °C in both samples (associated with weight losses of approximately 5%), and that total decomposition occurs above 450 °C, according to the behaviour of pure PVP [35].

3.2. Catalytic tests

3.2.1. Impregnated vs. nanoparticle-based catalysts

Fig. 4 reports the catalytic activity of sample Pd/A-4, as an example of the nanoparticle-based catalysts, and compares the results with the behaviour of the impregnated (i.e. standard) catalyst. It also includes the selectivity towards CO oxidation as a function of temperature. This figure clearly shows important differences between the impregnated and the nanoparticle-based

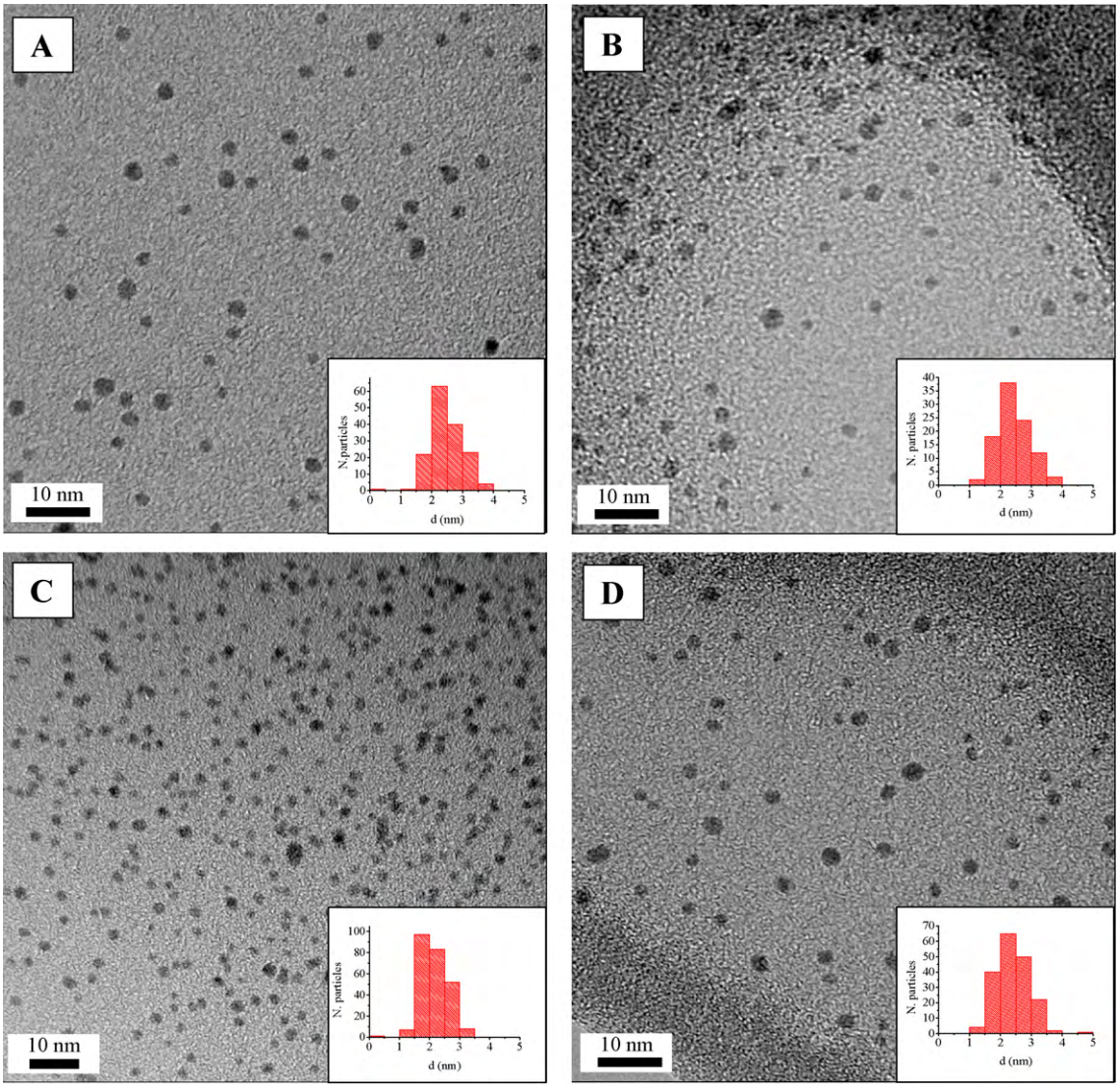

Fig. 1. TEM images of the following colloids: (A) Pd-1, (B) Pd-2, (C) Pd-3, (D) Pd-4. Scale bars are 10 nm in all cases. *Insets*: Particle size histograms based on a particle count of at least 100 elements.

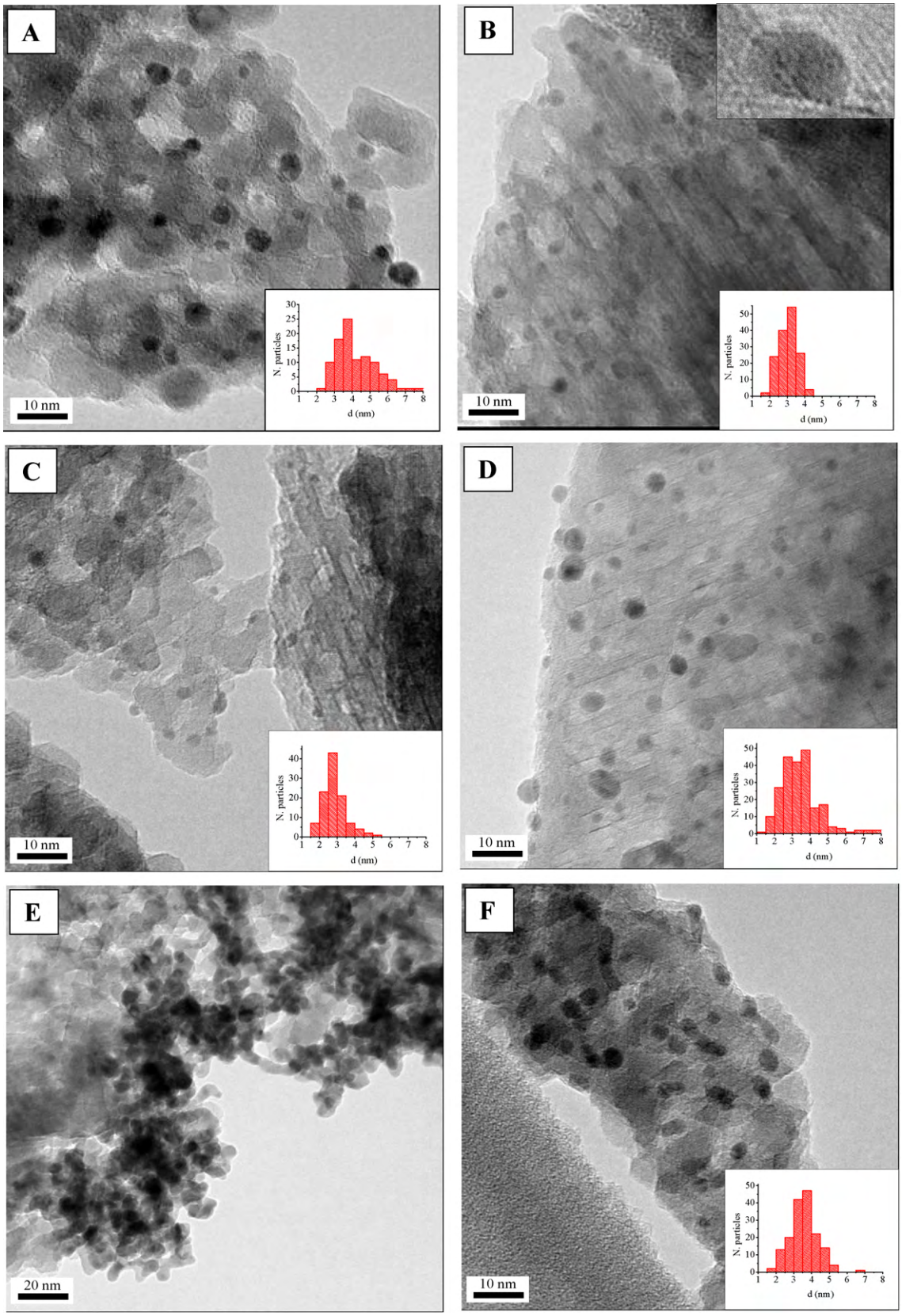

Fig. 2. TEM images of the following catalysts: (A) Pd/A-1, (B) Pd/A-2, (C) Pd/A-3, (D) Pd/A-4, (E) Pd/A-5, (F) Pd/A-6, (G) Pd/A-7, (H) Pd/A-Impregnation. Scale bars are 10 nm in all cases, except in E (20 nm). *Insets*: Particle size histograms based on a particle count of at least 100 elements.

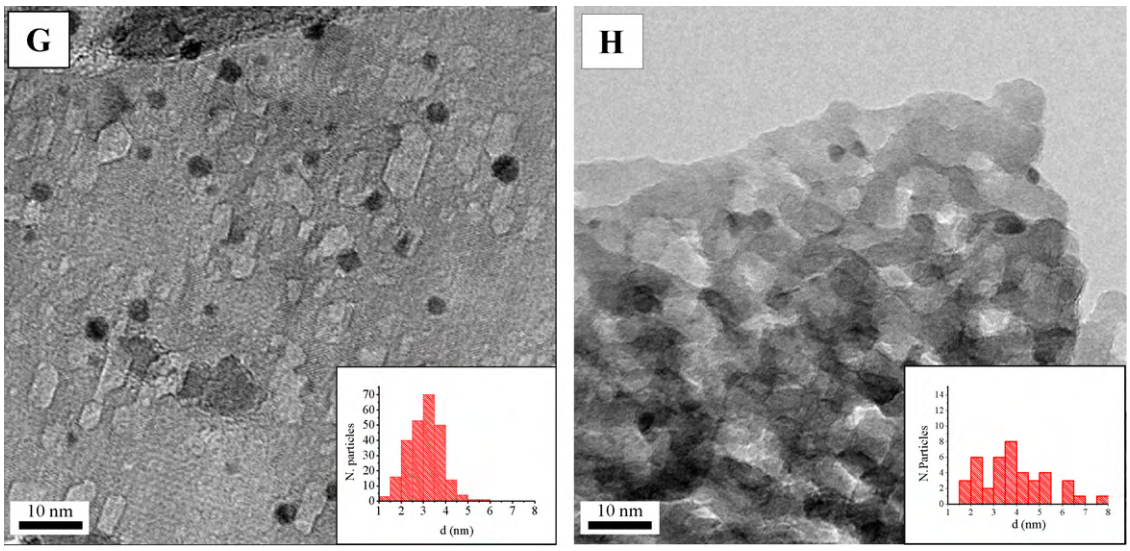

Fig. 2. (*Continued*).

catalyst. The impregnated catalyst is more active (the onset reaction temperature is about 30 °C lower with respect to the nanoparticle-based catalyst) but much less selective to CO oxidation. Thus, the maximum selectivity is about 10% for the impregnated catalyst (in agreement with other authors [41]), and reaches 50% for the nanoparticle-based catalyst.

The activation energy calculated from the isothermal experiments is 85 ± 20 kJ/mol for the impregnated catalyst and 165 ± 20 kJ/mol for the nanoparticle-based catalyst. Considering

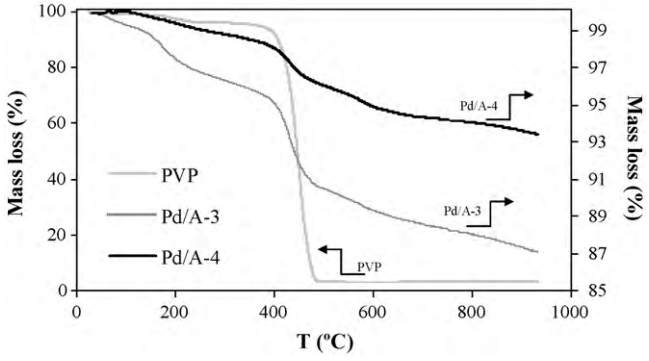

Fig. 3. Thermogravimetric analyses of pure PVP and colloidal catalysts (Pd/A-3 and Pd/A-4).

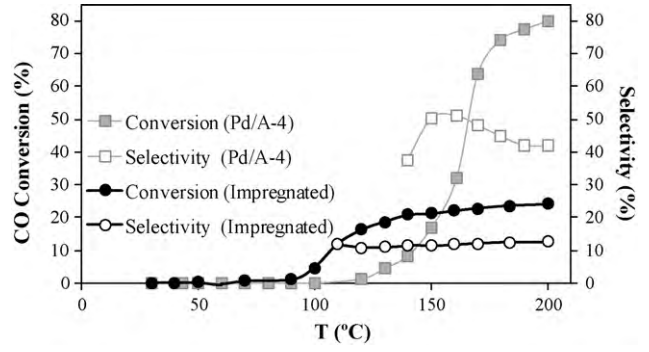

Fig. 4. Comparison of the catalytic activity (solid symbols) and selectivity (hollow symbols) of the impregnated and a nanoparticle-based (Pd/A-4) catalyst. Inlet feed composition: 2% CO, 2% O_2, 30% H_2, balance He. GHSV = 30,000 h^{-1}.

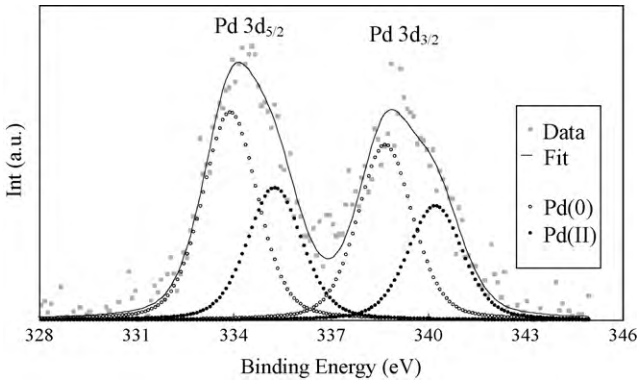

Fig. 5. X-ray photoelectron spectrum of catalyst Pd/A-4 after the reductive pre-treatment.

that the average particle size measured by TEM (Table 2) is similar in both cases and the different values of activation energy, the difference in selectivity is in agreement with an electronic effect produced by the presence of PVP as capping agent. The charge-transfer complex created through the carbonyl group of the PVP withdraws electron density from the Pd particle, which results in the affinity for CO by the nanoparticles surface being enhanced (in detriment of H_2 adsorption).

XPS analyses were performed on samples Pd/A-4 and Pd/A-Impregnation before and after the reductive pre-treatment. Fig. 5 includes the XPS spectrum of sample Pd/A-4 in the 3d region of Pd, and Table 3 shows the results of the analyses for the impregnated and the colloidal catalysts, including the atomic percentage of the different Pd species present in the samples. These data revealed the presence of two bands corresponding to the $3d_{3/2}$ and $3d_{5/2}$ transi-

Table 3
XPS analyses of the Pd/A-Impregnated and Pd/A-4 catalysts, before and after the reductive pre-treatment.

		BE Pd $3d_{5/2}$		Pd percentage	
		Fresh	Reduced	Fresh	Reduced
Pd/A-Impregnated	Pd(0)	333.8	334.0	50%	100%
	Pd(II)	335.3	–	50%	0%
Pd/A-4	Pd(0)	333.9	333.8	40%	61%
	Pd(II)	335.3	335.2	60%	39%

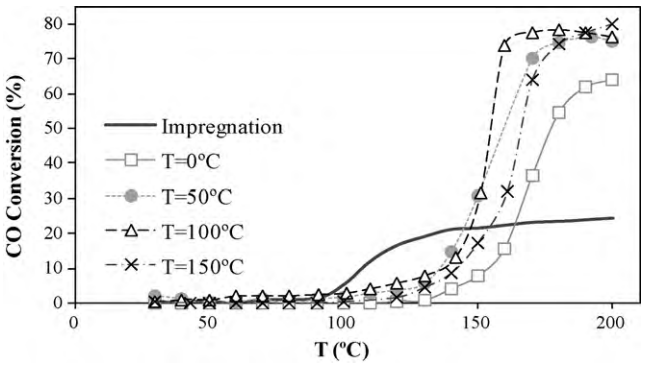

Fig. 6. Effect of the synthesis temperature on the catalytic performance of several nanoparticle-based catalysts. Results using the impregnated catalyst are shown for comparison purposes. Inlet feed composition: 2% CO, 2% O_2, 30% H_2, balance He. GHSV = 30,000 h^{-1}.

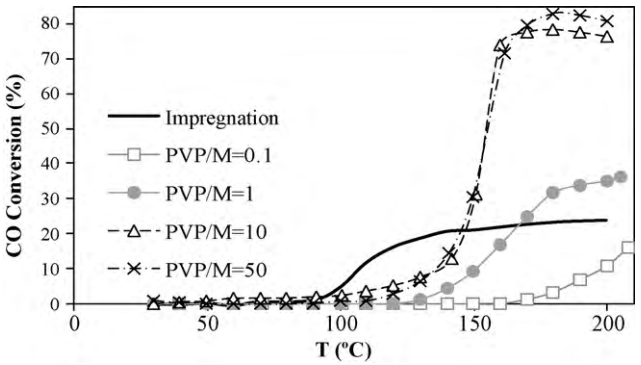

Fig. 7. Effect of the PVP/Pd ratio on the activity of Pd/Al_2O_3 samples synthesized at 100 °C. Inlet feed composition: 2% CO, 2% O_2, 30% H_2, balance He. GHSV = 30,000 h^{-1}.

tions. In the case of sample Pd/A-4 these bands were formed by two peaks each, which would in principle correspond to Pd(0) and Pd(II). A more detailed analysis of the binding energy of the peaks revealed that the peak appearing at higher binding energies (Pd(II)) could not be removed even after the reductive pre-treatment, and it was slightly shifted with respect to those of PdO (which should appear at approximately 336.7 and 342.3 eV, respectively). This could be attributed to the carbonyl function of the protecting polymer interacting with the metallic palladium, withdrawing electron density from its surface. This effect would cause a substantial shift in the binding energy at which the peak would appear, but not as high as to the peak appearing at the binding energy corresponding to PdO. This highlights the interaction between PVP and Pd, giving rise to the aforementioned electronic effect. However, for the impregnated catalyst no peaks at high binding energies are observed after the reductive pre-treatment, thus indicating the total reduction of the Pd species. This electronic effect has also been observed for platinum nanoparticles prepared using this kind of agent [35,42,43]. The substantial difference in the catalytic behaviour highlights the importance of using PVP as capping agent as well as the usefulness of the polyol reduction method.

However, other effects should not be ruled out. In this respect, nanoparticle size dispersity might be an important parameter affecting the catalytic activity of the analyzed samples. As Table 2 shows, the impregnated catalyst is the sample displaying the broadest particle size distribution and the largest average particle size. Our results indicate that this sample was the least selective in the PrOx reaction. This suggests that there is an optimum Pd nanoparticle size to carry out CO oxidation.

In the next sections, results obtained for catalysts obtained at different experimental conditions during the synthesis of the nanoparticles are presented.

3.2.2. *Effect of the nanoparticles synthesis temperature*

Fig. 6 shows the catalytic activity of samples Pd/A-1 to Pd/A-4, where the reduction temperature changed from 0 to 150 °C in 50 °C intervals. There seems to be a noticeable effect of the synthesis temperature over the catalytic activity of the samples, affecting both the CO conversion and the T_{50} of the catalytic process.

On the one hand, as the nanoparticle synthesis temperature is increased, T_{50} decreases, reaching a minimum value of ~160 °C for the samples prepared at 50 and 100 °C. On the other hand, CO conversion reaches values of around 75% in all cases except for sample Pd/A-1 synthesized at 0 °C. The slightly larger size of the palladium particles in this sample could be the explanation of this effect, which may be due to the temperature at which the nanoparticles are synthesized. Considering the glass transition temperature (T_g) of PVP (between 110 and 180 °C depending on the cross-linking between the chains and the average polymer weight), at low temperatures the polymer chains may be too stiff to efficiently coat the surface of the nanoparticles by binding their carbonyl groups to the surface Pd atoms. This effect would be more pronounced as the temperature is decreased, in agreement with our results. On the other hand, when the synthesis temperature approaches T_g, the protective effect of the PVP is enhanced from the presence of more flexible polymer chains. Nevertheless, too high synthesis temperatures may hinder such effect. At high reduction temperatures, the Pd reduction rates (and hence the kinetics of nanoparticle growth) are too fast for the polymer chains to wrap themselves around the forming nanoparticles, not being able to prevent their further growth. A compromise solution must be reached in order to reach the optimum synthetic conditions, which in our case seems to be the synthesis of nanoparticles at 100 °C.

3.2.3. *Effect of the PVP/Pd ratio*

Several studies have analyzed the role of the capping agent in nanoparticle synthesis [13,40] as well as the influence of the amount of capping agent on the final nanoparticle size and the resulting catalytic activity. Thus, we have studied this effect by preparing different colloids with PVP/Pd ratios ranging from 0.1 to 50 and submitting the prepared catalysts to the PrOx reaction. From Fig. 7, the effect of the capping agent on the catalytic activity of the catalysts can be inferred. The PVP/Pd ratio employed during the synthesis of the nanoparticles has a marked effect on the catalytic activity of the corresponding catalysts (samples Pd/A-5, Pd/A-6, Pd/A-3, and Pd/A-7 were prepared using PVP/Pd ratios of 0.1, 1, 10, and 50, respectively). For instance, sample Pd/A-5 shows a rather poor catalytic activity, which is a direct consequence of the big aggregates formed on the surface of the catalyst due to the lack of protecting polymer, as shown in the TEM micrographs (Fig. 2E). Increasing the concentration of PVP when synthesizing the nanoparticles results in a substantial improvement of the resulting catalytic activity until a PVP/Pd value of 10 is reached, point after which no improvement is observed, even when the concentration of PVP is increased five-fold.

As Somorjai and co-workers already pointed out in various papers on Pt nanoparticles [35,42,43], PVP protects the newly formed nanoparticle, avoiding its oxidation/agglomeration by binding to its surface via the carbonyl groups in the pyrrolidone ring. This binding creates a charge-transfer complex which withdraws electron density from the Pt particle, thus modifying its catalytic activity. From our results it appears that the catalytic performance is improved as you increase the number of carbonyl groups interacting with the Pd nanoparticles. This electronic effect may explain the much higher selectivity of the nanoparticle-based catalysts compared to the impregnated catalyst. Although we have

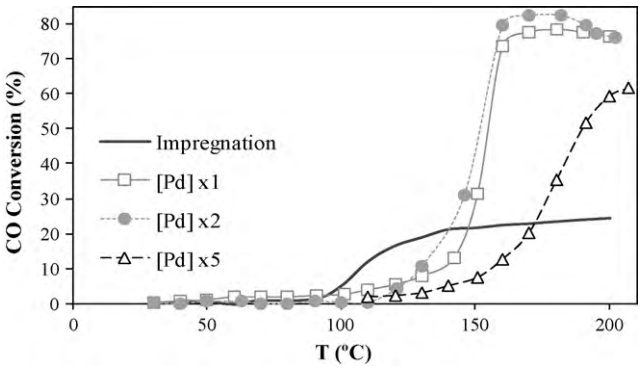

Fig. 8. Effect of initial Pd concentration on the activity of catalysts synthesized at 100 °C. Inlet feed composition: 2% CO, 2% O_2, 30% H_2, balance He. GHSV = 30,000 h^{-1}.

not quantified the number of carbonyls, a PVP/Pd ratio of 10 seems to be the optimum value. Furthermore, temperatures close to T_g of the capping agent may favour the formation of a greater number of carbonyl-Pd links, thus improving the catalytic performance.

3.2.4. Effect of the metal concentration

Palladium concentration in the initial colloid solution was also a parameter analyzed in order to obtain a better understanding of the parameters affecting the catalytic performance of the catalysts in the PrOx reaction. These solutions were prepared by reducing the amount of solvent by two and five times with respect to the procedure described in Section 2.

The results corresponding to the performance of the catalysts using different Pd concentrations are shown in Fig. 8: sample Pd/A-3 was synthesized as described in the experimental section; for samples Pd/A-8 and Pd/A-9 the initial Pd concentrations were two and five times higher than Pd/A-3, respectively. Increasing the initial concentration by a factor of 2 only seems to have a slight effect over the maximum CO conversion, as well as the T_{50}. However, when the initial Pd concentration is increased five-fold, dramatic changes can be appreciated on the catalyst performance, with T_{50} being increased in ~30 °C, and maximum CO conversion barely reaching 60% at these experimental conditions.

This behaviour may be once again explained in terms of size of the palladium nanoparticles. The apparent decrease in activity at temperatures above 180 °C of sample Pd/A-8, i.e. that prepared with a two times higher concentration of Pd, is in agreement with the observations reported by Oh and Sinkevich [44], who attributed this behaviour to the water-gas shift reaction becoming more relevant together with desorption of CO from the catalyst surface at higher temperatures.

As it was observed when the influence of the synthesis temperature was analyzed (see Section 3.2.2), large Pd particles seem to negatively affect the performance of the catalysts in the PrOx reaction, being the optimum value 2.2 nm for the Pd nanoparticles size in the colloid, and a size between 2.5 and 3.5 nm for the supported nanoparticles. This once again highlights the influence of the catalyst average particle size dispersity on the catalytic activity, as pointed out in Section 3.2.1.

3.2.5. Catalytic performance in the presence of CO_2 and H_2O

In this section, the catalytic activity at different space velocities and in presence of CO_2 and H_2O is presented, in order to analyze the usefulness of these catalysts for the PrOx reaction.

In the PrOx reaction, H_2 oxidation occurs as a side reaction to a certain extent, generating H_2O in the reactor, which could be an important drawback from both a technological and economical point of view. Thus, selectivity is a parameter of paramount importance in the PrOx reaction in H_2-rich streams.

Table 4
Catalytic results in the PrOx reaction. T_{50} and maximum selectivity (from the non-isothermal experiments) are specified for each sample (temperature corresponding to the maximum selectivity is indicated in brackets). Reaction rates and TOF (calculated at 150 °C) are also indicated.

Sample	T_{50} (°C)	Maximum selectivity (%)	TOF (s^{-1})	Reaction rate (mol/s g Pd)
Pd/A-1	180	42 (170 °C)	0.08	1.6×10^{-4}
Pd/A-2	160	56 (150 °C)	0.18	5.1×10^{-4}
Pd/A-3	155	47 (160 °C)	0.28	8.4×10^{-4}
Pd/A-4	165	51 (160 °C)	0.10	2.4×10^{-4}
Pd/A-5	–[a]	17 (200 °C)	–[b]	–[b]
Pd/A-6	–[a]	26 (150 °C)	0.11	2.5×10^{-4}
Pd/A-7	155	55 (150 °C)	0.25	7.0×10^{-4}
Pd/A-8	150	56 (145 °C)	0.26	6.8×10^{-4}
Pd/A-9	190	37 (150 °C)	0.11	2.1×10^{-4}
Pd/A-Impregnation	–[a]	13 (200 °C)	0.20	4.4×10^{-4}

[a] These samples do not reach 50% CO conversion.
[b] No catalytic activity was detected for this sample at 150 °C.

The selectivity of the samples was also analyzed during the catalytic tests. Table 4 includes the maximum selectivity of the catalysts in this work, and the reaction rates and TOF for each sample.

The palladium "standard" impregnated catalyst is the sample showing the lowest selectivity, being useless for PrOx reaction. However, the maximum selectivity for the nanoparticle-based catalyst is, in most cases, above 40% (above 50% in some cases), being of great interest for this reaction. In order to check the possibility of using these catalysts for the complete removal of CO, additional experiments were carried out at lower space velocity. Fig. 9 includes the catalytic activity of catalyst Pd/A-4 at lower space velocity with the standard feed (i.e. 2% CO, 2% O_2, 30% H_2 in He). It can be observed that 100% CO conversion can be reached at ~160 °C, which is an outstanding observation. Since the reaction feed contains CO_2 and H_2O that may contribute to additional reactions, the suitability of the catalysts for this reaction must be studied in presence of these compounds. Fig. 9 also shows the activity of the same catalyst with H_2O and CO_2 in the gas mixture. Although the activity is slightly reduced, 100% conversion of CO can be reached at a temperature around 180 °C.

From our results, CO_2 and water vapour do not affect significantly the catalytic performance of the colloidal catalyst, although a slight shift towards higher T_{50} is observed for the sample tested under more realistic conditions. This is in good agreement with the findings obtained by other authors for Cu/CuO–CeO_2 and Au/Fe_2O_3 systems, although they show a more marked shift when CO_2 and H_2O are fed into the reactor [45,46]. Furthermore, sample Pd/A-4 shows a higher tolerance under realistic conditions than other catalysts which exhibit a substantial loss of activity when tested under CO_2/H_2O atmosphere [47–49]. Due to the behaviour of these

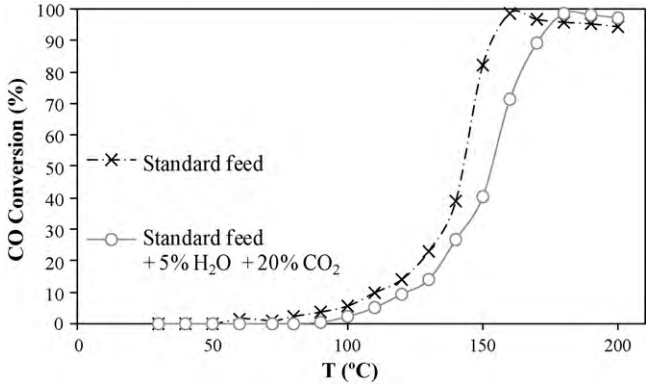

Fig. 9. Effect of CO_2 and water vapour on the catalytic activity of sample Pd/A-4. Standard feed composed by 2% CO, 2% O_2, 30% H_2, balance He. GHSV = 10,000 h^{-1}.

catalysts under realistic working conditions, these materials seem to be very promising for the development of active and selective catalysts for the PrOx reaction.

If we are to critically compare our results with those found in the literature for catalytic systems using different metals, one should first consider that a substantial number of the already published data deal with the oxidation of CO in H_2-free streams [50–53]. In these cases the matter of the selectivity is not addressed. Nevertheless, some of those works have reported very efficient catalysts for the oxidation of CO at very low temperatures based on noble metal systems supported on a wide range of transition metal oxides [21,41,53,54]. However, the adequate temperature range for an integrated hydrocarbon reformer-fuel cell system is between 100 and 200 °C. Furthermore, the presence of a high concentration of H_2 must be taken into account. This has driven several research groups to shift from Au to other metals that may withstand those working conditions. Of all the metals tested, group 9 and 10 metals (mainly Pt) seem to yield the most promising results [44,47,55]. Substantial efforts have been dedicated to the testing of supported Pt catalysts prepared by standard or colloidal techniques [55–57].

Gold catalysts have recently been the focus of many different works related to CO oxidation, since this metal has been proven to be very active [58] and selective [59] for this reaction at low temperatures [17,21]. However, recent results have shown that gold strongly deactivates when working for several hours, or at moderately high temperatures [21], thus not being appropriate to use as PrOx catalysts.

Pd seems to have fallen behind in terms of research efforts, partly due to the results obtained with the resulting catalysts prepared by classical impregnation methods [47]. In contrast, our results clearly show that PVP-capped Pd nanoparticles prepared by the reduction-by-solvent method constitute a very promising system for CO abatement in H_2-rich streams, compared to other Pd [41,47,60] or other metal (Pt, Ir) catalysts [60] present in literature. Furthermore, these catalysts are highly selective in the PrOx reaction as compared to those reported in the literature for different systems (Pt particles [60–62], Au particles [63], Pd over different inorganic solids [41]), with selectivities reaching values as high as 50%.

Additionally, all catalysts showed good stability over relatively long reaction times (6 h) at their maximum corresponding CO conversions with activity losses under 5%. Reaction rate values presented in this study are in the range of those found by other authors for platinum [64–66] catalysts. The results presented in this study where obtained using an inert support with no residual CO conversion (results not shown). Other authors have highlighted the importance of the support in the catalyst performance [52,65]. For instance, Hoflund et al. [67] observed that MnO_x was an excellent support for Au catalysts, obtaining substantially better results than Pt/SnO_x systems. It has been reported that partially reducible oxides are very promising supports for noble metal catalysts in the PrOx reaction [19,68,69], and further efforts will be carried out in our group in this direction.

4. Conclusions

Supported Pd catalysts have been prepared on an alumina support following two approaches: a classical approach in which $Pd(ac)_2$ was impregnated and reduced, and a colloidal approach in which metallic Pd nanoparticles were first synthesized and subsequently deposited. Most of the colloidal catalysts, when applied to the PrOx reaction (i.e. preferential oxidation of CO in the presence of large quantities of H_2) have shown good catalytic behaviour. In this respect, impregnated Pd catalysts perform very poorly in this particular reaction. One of the key aspects of this work lies in the importance of the use of PVP as capping agent due to the formation of a charge-transfer complex which, by delocalizing the electron density on the Pd nanoparticle, greatly improves the performance of the catalyst. In this respect, both the amount of capping agent (represented by the PVP/Pd molar ratio) and the temperature at which the nanoparticles are synthesized are key factors in the preparation process. From our observations, the optimum values are 10 and 100 °C, respectively. Another important parameter is the average particle size and its dispersity in the catalyst. It has been observed that the best catalysts are those with a small average particle size of approximately 2.5–3 nm and a narrow particle size distribution.

Our results show that colloidal Pd nanoparticles supported on alumina convert CO to CO_2 efficiently and with very high selectivity in the PrOx reaction (above 50% in some cases) with no significant loss of activity for several hours. In addition, complete CO removal can be achieved even when the catalysts are tested under CO_2 and H_2O atmosphere, simulating real conditions of application of these new materials. As a result, these catalysts may be considered highly promising for the development of hydrogen purification devices for potential fuel cell applications.

Acknowledgements

The authors would like to thank the Spanish Ministerio de Ciencia e Innovación (MICINN), PLAN E funds and FEDER program (Projects CTQ2009-10813/PPQ, CTQ2006-08958, RyC-2009-03813), as well as the PROMETEO project (Prometeo/2009/047) from the Generalitat Valenciana for the financial support for this work.

References

[1] F. Porta, M. Rossi, J. Mol. Catal. A 204 (2003) 553–559.
[2] Y. Shiraishi, N. Toshima, J. Mol. Catal. A 141 (1999) 187–192.
[3] N. Yan, C. Zhao, C. Luo, P.J. Dyson, H. Liu, Y. Kou, J. Am. Chem. Soc. 128 (2006) 8714–8715.
[4] P. Lu, T. Teranishi, K. Asakura, M. Miyake, N. Toshima, J. Phys. Chem. B 103 (1999) 9673–9682.
[5] B.F.G. Johnson, Top. Catal. 24 (2003) 147–159.
[6] M.A. El-Sayed, Acc. Chem. Res. 37 (2004) 326–333.
[7] G.A. Somorjai, J.Y. Park, Top. Catal. 49 (2008) 126–135.
[8] T.D. Schladt, T. Graf, W. Tremel, Chem. Mater. 21 (2009) 3183–3190.
[9] R. Narayanan, M.A. El-Sayed, Nano Lett. 4 (2004) 1343–1348.
[10] J.Y. Park, C. Aliaga, J.R. Renzas, H. Lee, G.A. Somorjai, Catal. Lett. 129 (2009) 1–6.
[11] C. Kim, H. Lee, Catal. Comm. 10 (2009) 1305–1309.
[12] J. Haber, J.H. Block, B. Delmon, Pure Appl. Chem. 67 (1995) 1257–1306.
[13] P.S. Roy, J. Bagchi, S.K. Bhattacharya, Trans. Met. Chem. 34 (2009) 447–453.
[14] R. Farrauto, S. Hwang, L. Shore, W. Ruettinger, J. Lampert, T. Giroux, Y. Liu, O. Ilinch, Annu. Rev. Mater. Res. 33 (2003) 1–27.
[15] J.D. Holladay, J. Hu, D.L. King, Y. Wang, Catal. Today 139 (2009) 244–260.
[16] O. Korotkikh, R. Farrauto, Catal. Today 62 (2000) 249–254.
[17] M. Haruta, T. Kobayashi, H. Sano, N. Yamada, Chem. Lett. 2 (1987) 405–408.
[18] D.T. Thompson, Gold Bull. 31 (1998) 111–118.
[19] B. Quiao, L. Liu, J. Zhang, Y. Deng, J. Catal. 261 (2009) 241–244.
[20] M.M. Schubert, S. Hackenberg, A.C. van Veen, M. Muhler, V. Plzak, R.J. Behm, J. Catal. 197 (2001) 113–122.
[21] B. Schumacher, Y. Denkwitz, V. Plzak, M. Kinne, R.J. Behm, J. Catal. 224 (2004) 449–462.
[22] H. Zhang, X. Hu, Sep. Purif. Technol. 34 (2004) 105–108.
[23] U. Heiz, A. Sanchez, S. Abbet, W.-D. Schneider, J. Am. Chem. Soc. 121 (1999) 3214–3217.
[24] M. Chen, L. Qi, X. Zheng, Kinet. Catal. 49 (4) (2008) 493–498.
[25] W.Y. Pong, H.Y. Chang, H.I. Chen, J.R. Chang, Surf. Rev. Lett. 15 (1&2) (2008) 123–131.
[26] M.S. Chen, Y. Cai, Z. Yan, K.K. Gath, S. Axnanda, D. Wayne Goodman, Surf. Sci. 601 (23) (2007) 5326–5331.
[27] M.E. Grass, S.H. Joo, Y. Zhang, G.A. Somorjai, J. Phys. Chem. C 113 (2009) 8616–8623.
[28] N. Toshima, M. Harada, Y. Yamazaki, K. Asakura, J. Phys. Chem. 96 (1992) 9927–9933.
[29] S. Domínguez-Domínguez, Á. Berenguer-Murcia, D. Cazorla-Amorós, Á. Linares-Solano, J. Catal. 243 (2006) 74–81.
[30] S. Domínguez-Domínguez, Á. Berenguer-Murcia, B.K. Pradhan, Á. Linares-Solano, D. Cazorla-Amorós, J. Phys. Chem. C 112 (2008) 3827–3834.

[31] S. Domínguez-Domínguez, Á. Berenguer-Murcia, Á. Linares-Solano, D. Cazorla-Amorós, J. Catal. 257 (2008) 87–95.
[32] G.K. Bethke, H.H. Kung, Appl. Catal. A 194–195 (2000) 43–53.
[33] I.H. Son, M. Shamsuzzoha, A.M. Lane, J. Catal. 210 (2002) 460–465.
[34] E. Moretti, M. Lenarda, L. Storaro, A. Talon, R. Frattini, S. Polizzi, E. Rodríguez-Castellón, A. Jiménez-López, Appl. Catal. B 72 (2006) 149–156.
[35] Y. Borodko, S.E. Habas, M. Koebel, P. Yang, H. Frei, G.A. Somorjai, J. Phys. Chem. B 110 (2006) 23052–23059.
[36] M. Boudart, Kinetics of Heterogeneous Catalytic Reactions, Princeton University Press, Princeton, NJ, 1984.
[37] P. Naknam, A. Luengnaruemitchai, S. Wongkasemjit, S. Osuwan, J. Power Sources 165 (2007) 353–358.
[38] T. Caputo, L. Lisi, R. Pirone, G. Russo, Ind. Eng. Chem. Res. 46 (2007) 6793–6800.
[39] C. Vázquez-Vázquez, M. Bañobre-López, A. Mitra, M.A. López-Quintela, J. Rivas, Langmuir 25 (2009) 8208–8216.
[40] L. Kemal, X.C. Jiang, K. Wong, A.B. Yu, J. Phys. Chem. C 112 (2008) 15656–15664.
[41] N. Iwasa, S. Arai, M. Arai, Appl. Catal. B 79 (2008) 132–141.
[42] Y. Borodko, S.M. Humphrey, T.D. Tilley, H. Frei, G.A. Somorjai, J. Phys. Chem. C 111 (2007) 6288–6295.
[43] J.K. Navin, M.E. Grass, G.A. Somorjai, A.L. Marsh, Anal. Chem. 81 (2009) 6295–6299.
[44] S. Oh, R.M. Sinkevich, J. Catal. 142 (1993) 254–262.
[45] G. Avgouropoulos, T. Ioannides, H.K. Matralis, J. Batista, S. Hocevar, Catal. Lett. 73 (1) (2001) 33–40.
[46] G. Avgouropoulos, T. Ioannides, Ch. Papadopoulou, J. Batista, S. Hocevar, H.K. Matralis, Catal. Today 75 (2002) 157–167.
[47] S. Zhou, Z. Yuan, S. Wang, Int. J. Hydrogen Energ. 31 (2006) 924–933.
[48] G. Avgouropoulos, M. Manzoli, F. Boccuzzi, T. Tabakova, J. Papavasiliou, T. Ioannides, V. Idakiev, J. Catal. 256 (2008) 237–247.
[49] C.Y. Shiau, M.W. Ma, C.S. Chuang, Appl. Catal. A 301 (2006) 89–95.
[50] V. Abdelsayed, A. Aljarasah, M.S. El-Shall, Z.A. Al-Othman, A.H. Alghamdi, Chem. Mater. 21 (1) (2009) 2825–2834.
[51] Z. Wu, S. Zhou, H. Zhu, S. Dai, S.H. Overbury, J. Phys. Chem. C 113 (2009) 3726–3734.
[52] E.M.C. Alayon, J. Singh, M. Nachtegaal, M. Harfouche, J.A. van Bokhoven, J. Catal. 263 (2009) 228–238.
[53] X. Xie, Y. Li, Z. Liu, M. Haruta, W. Shen, Nature 458 (2009) 746–749.
[54] M. Date, M. Oukumura, S. Tsubota, M. Haruta, Angew. Chem. Intl. Ed. 43 (2004) 2129–2132.
[55] A. Manasilp, E. Gulari, Appl. Catal. B 37 (2002) 17–25.
[56] B. Atalik, D. Uner, J. Catal. 241 (2006) 268–275.
[57] S.Y. Chin, O.S. Alexeev, M.D. Amiridis, J. Catal. 243 (2006) 329–339.
[58] E.Y. Ko, E.D. Park, K.W. Seo, H.C. Lee, D. Lee, S. Kim, Catal. Today 116 (2006) 377–383.
[59] M.C. Schubert, A. Venugopal, M.J. Kahlich, V. Plzak, R.J. Behm, J. Catal. 222 (2004) 32–40.
[60] F. Mariño, C. Descorme, S. Duprez, Appl. Catal. B 54 (2004) 59–66.
[61] I. Rosso, C. Galletti, G. Saracco, E. Garrone, V. Specchia, Appl. Catal. B 48 (2004) 195–203.
[62] F. Wang, G. Lu, J. Power Sources 181 (2008) 120–126.
[63] C. Rossignol, S. Arrii, F. Morfin, L. Piccolo, V. Caps, J.L. Rousset, J. Catal. 230 (2005) 476–483.
[64] J.A. Rodriguez, D.W. Goodman, Surf. Sci. Rep. 14 (1991) 1–107.
[65] N.W. Cant, J. Catal. 62 (1980) 173–175.
[66] N.W. Cant, P.C. Hicks, B.S. Lennon, J. Catal. 54 (1978) 372–383.
[67] G.B. Hoflund, S.D. Gardner, D.R. Schryer, B.T. Upchurch, E.J. Kielin, Appl. Catal. B 6 (1995) 117–126.
[68] A. Iglesias-Juez, A.B. Hungría, A. Martínez-Arias, J.A. Anderson, M. Fernández-García, Catal. Today 143 (2009) 195–202.
[69] P. Landon, J. Ferguson, B.E. Solsona, T. Garcia, A.F. Carley, A.A. Herzing, C.J. Kiely, S.E. Golunksi, G.J. Hutchings, Chem. Comm. 27 (2005) 3385–3387.